Proceedings of the 21st ICSMGE, Vienna, Austria, 14 – 19 June 2026. Pistrol, Adam & Schweiger (eds.)
Published by: ÖGG, Austrian Society for Geomechanics, Salzburg, Austria, ISBN 978-3-9503898-4-5
https://doi.org/10.53243/ICSMGE2026-369

Multi-Scale Experimental Investigation of Soil-Abutment Interaction in Integral Bridges Under Cyclic Thermal Loading

Sha Luo
Mott MacDonald, Birmingham, UK, sha.luo@MottMac.com
School of Engineering, University of Birmingham, UK, s.luo@bham.ac.uk

Nicole Metje, David Chapman, Christopher D.F. Rogers
School of Engineering, University of Birmingham, UK

Raffaele De Risi, Ziyan Huang, Flavia De Luca
School of Civil, Aerospace and Design Engineering, University of Bristol, UK

David Milne, William Powrie
School of Engineering, University of Southampton, Southampton, UK

George Mylonakis
University of Bristol, UK & College of Engineering, Khalifa University, UAE

Anastasios Sextos
University of Bristol, UK & National Technical University of Athens, Greece

ABSTRACT: Integral Abutment Bridges (IABs) are widely adopted in modern infrastructure due to their construction simplicity and reduced maintenance relative to ordinary bridges. However, their long-term performance remains uncertain due to the complex soil-structure interaction (SSI) effects under seasonal cyclic thermal loading. This study investigates the evolution of lateral earth pressures and backfill densification through a coordinated multi-scale (large and small) experimental programme and numerical modelling. Small-scale 1g tests and large-scale physical experiments were conducted at the University of Bristol's Soil Foundation Structure interaction laboratories (SoFSI) and the Earthquake and Large Structures (EQUALS) facilities, simulating thermal expansion and contraction over up to 120 cycles. Results reveal a progressive increase in lateral earth pressure, driven by cyclic densification of the backfill—particularly near rigid abutments. Peak pressure locations were observed to shift with loading cycles, closely associated with local compaction patterns captured using Ground Penetrating Radar (GPR) and Particle Image Velocimetry (PIV). Complementary numerical simulations using different computational platforms (PLAXIS, ABAQUS, and OpenSees) reproduced key behavioural trends and confirmed the critical influence of abutment stiffness, displacement amplitude, and cumulative loading. Compared with static predictions from analytical methods and design guidelines (e.g. PD6694-1), the herein reported experimental and numerical results demonstrate significantly higher lateral pressures, underscoring the limitations of current design assumptions. By bridging small-scale precision, large-scale realism, and numerical insight, this study advances the understanding of SSI in IABs under realistic thermal loads. The findings provide a foundation for improving design practices to ensure the long-term resilience and reliability of integral bridges.

KEYWORDS: Integral Abutment Bridges (IABs), Soil-Structure Interaction (SSI), Cyclic Thermal Loading, Multi-Scale Experiments.

1 INTRODUCTION

1.1 *Background on Integral Abutment Bridges (IABs)*

Integral abutment bridges (IABs) have become an increasingly preferred solution for short- to medium-span bridges due to the elimination of expansion joints and bearings, which significantly reduces maintenance demands and improves long-term durability (England et al., 2000; Burke, 2009; Luo et al., 2022). IABs rely on the interaction between the bridge deck and surrounding backfill to accommodate thermal expansion and contraction, leading to the development of complex soil–structure interaction phenomena (Barker and Carder, 2000; Tapper and Lehane, 2004). Long-term cyclic thermal loading introduces cumulative effects in the backfill, such as soil densification and stiffness changes, which are not yet fully accounted for in current design methods (Lehane, 2011; Luo et al., 2022, 2023, 2025).

Previous studies in the area have employed physical modelling, numerical simulations (Ravjee et al., 2018; Xu & Guo, 2021), and field monitoring (Lawver et al., 2000; LaFave et al., 2021). However, a unified understanding across different specimen scales remains lacking. This calls for an integrated approach that combines small-scale and large-scale experiments, in-situ observations, and numerical modelling to support performance-based design and guide future code development.

1.2 *Limitations of Current Design Guidance (PD 6694-1)*

The UK guidance document PD 6694-1:2011 (BSI, 2011) provides recommendations for the design of IABs, including limitations on the maximum allowable bridge length (60 m) and maximum skew angle (30°) due to concerns over the development of excessive lateral earth pressures and associated deck–abutment interaction. These limitations are primarily based on conservative assumptions and simplified soil models, which may not fully reflect the observed behaviour from recent field studies and physical testing (Mark, 2013; Luo et al., 2025).

Furthermore, PD 6694-1 assumes a linear pressure distribution and constant soil properties over time, neglecting the cumulative densification observed in granular backfill under

cyclic loading. This simplification can lead to inaccuracies in stress prediction and substructure design, particularly for bridges exposed to frequent temperature variations (Fleming & Rogers, 1995; Diceli & Erhan, 2010; Luo et al., 2025).

1.3 *Thermal Loading Effects and Lateral Earth Pressure Development*

Cyclic thermal expansion and contraction in IABs induce progressive densification of the backfill and significant development of lateral earth pressures on the abutment (Springman et al., 1996; Tapper & Lehane, 2004; Luo et al., 2022). Field observations and centrifuge tests have confirmed that repeated temperature fluctuations tend to intensify soil compaction and shift lateral pressure distributions (Lawver et al., 2000; LaFave et al., 2021). Despite this, current design codes overlook these cumulative effects and, instead, assume constant soil properties. Recent laboratory studies, employing distributed fibre optic sensing, captured evolving strain and pressure profiles under thermal cycling (Luo et al., 2025), while advanced numerical models (e.g., PLAXIS, ABAQUS and Opensees) simulated the associated stress–strain evolution, reinforcing the need to integrate computational and physical evidence for reliable IAB design (Khodair & Hassiotis, 2005; Caristo et al., 2018; Liu et al., 2022; Luo et al., 2023, Huang et al. 2025).

1.4 *Research Gap and Need for Multi-Scale Validation*

While substantial progress has been achieved through small-scale laboratory experiments, large-scale testing, and advanced numerical simulations, a critical lack of cohesive synthesis across these approaches remains. Comparative validation between different modelling scales is limited, especially regarding cyclic performance, backfill densification, and abutment displacement. Moreover, current design guidance (e.g., PD 6694-1) lacks calibration against distributed strain sensing data and does not fully account for the cumulative effects of thermal cycling or soil-structure interaction mechanisms observed in parametric modelling. This study addresses these gaps through a multi-scale investigation, bridging experimental and numerical insights to support design refinement.

1.5 *Multi-Scale Insights for Design Code Advancement*

A comparative synthesis of multiple complementary experimental campaigns is reported, spanning small-scale models, large-scale laboratory setups, field-monitored tests, and ground-penetrating radar (GPR) investigations, to evaluate the effects of cyclic thermal loading on integral abutment bridges. These findings are interpreted alongside validated numerical simulations using ABAQUS, PLAXIS and OpenSees to provide a unified evidence base. By capturing the evolution of soil-structure interaction mechanisms across different scales and modelling frameworks, this paper aims to critically assess and propose refinements to the PD 6694-1 design guidance, with a particular focus on cumulative deformation behaviour, lateral pressure development, and backfill densification. The aim of this study is to synthesise multi-scale evidence to understand soil-structure interaction under thermal cycling and to identify where PD 6694-1 (BSI, 2011) may require refinement.

2 EXPERIMENTAL PROGRAMME AND METHODOLOGIES

To investigate the cumulative effects of seasonal thermal loading on soil-abutment interaction in Integral Abutment Bridges (IABs), a coordinated experimental programme was conducted at two physical scales. The research integrated small-scale 1g model tests and large-scale physical simulations, each designed to isolate and characterise the development of lateral earth pressures, soil densification, and wall displacement under repeated thermal cycles. All experiments were conducted using dry uniform sand to eliminate the complexity of moisture-dependent variables and focus on stress-strain responses associated with thermal-induced cyclic movements.

2.1 *Small-Scale Physical Models (1g)*

The small-scale 1-metre-cube experiments were performed using a well-instrumented natural gravity (1g) setup designed to simulate thermal expansion and contraction effects (Figure 1b). The test chamber was filled with dry sand compacted in controlled layers behind a model abutment. Cyclic horizontal displacements were applied via an actuator to replicate seasonal deck movements. The rig (Figure 1a) incorporated earth pressure cells, linear variable differential transformers (LVDTs), and a non-metallic rig design to enable GPR measurements. A transparent Perspex side wall allowed particle image velocimetry (PIV) to capture both global and local deformation behaviour. A series of tests were conducted using Leighton Buzzard sand and varying abutment wall stiffnesses, enabling systematic investigation of their effects on soil–structure interaction under thermal cycles.

2.2 *Large-Scale Soil Pit Experiment*

To validate the small-scale findings and examine potential scaling effects, a large-scale test was conducted on a 3 m-high reinforced concrete abutment wall retaining approximately 35 m^3 of dry sand (Figure 1Figure 1c). The abutment was subjected to cyclic horizontal loading via hydraulic jacks to simulate a 120-year service life under seasonal thermal movements. The test setup featured an extensive instrumentation array, including embedded pressure cells, strain gauges, laser LVDTs (Figure 1e), accelerometers and distributed optical fibre cables (Figure 1d)(along the wall face and within the backfill). This configuration enabled comprehensive monitoring of the stress evolution and deformation behaviour throughout the experiment.

2.3 *Use of GPR for Backfill Monitoring and Distributed Optical Fibre for Strain Monitoring of the Abutment Wall*

In both small- and large-scale tests, conventional sensors were installed to monitor key geotechnical and structural responses during cyclic loading. Earth pressure cells were mounted along the abutment wall to capture lateral earth stress distributions, while LVDTs and laser displacement sensors were positioned at critical locations to track wall displacement and backfill surface settlement. Accelerometers were embedded in the backfill to detect changes in stiffness during cyclic loading. Strain gauges were applied to the abutment wall to measure localised structural response. These traditional monitoring systems provided baseline measurements that were later complemented by advanced sensing techniques such as ground-penetrating radar (GPR) and distributed optical fibre sensors.

Since the velocity of GPR signals varies between air and soil due to their differing dielectric properties, any changes in the void ratio within the backfill - such as progressive densification or void formation - will alter the signal travel time for any fixed distance. By monitoring variations in travel time during the thermal loading cycles, the local dielectric permittivity can be inferred and used to estimate changes in backfill density. This back-analysis approach enables a non-invasive assessment of the evolving internal condition of the backfill behind the abutment.

To monitor the structural response of the abutment wall, distributed optical fibre sensing was employed by bonding fibres along the rear face of the concrete abutment. This technique enabled high-resolution, real-time strain measurements along the full height of the wall, capturing both transient and cumulative strain developments over successive thermal cycles. Unlike conventional strain gauges which may fail beyond the elastic range, optical fibres maintain functionality. Their durability and ease of installation make them highly suitable for field deployment and integration during infrastructure construction.

These datasets were cross-referenced with pressure cell and strain gauge outputs, reinforcing the observed trends and supporting the calibration of numerical models. This combined approach provided a robust foundation for interpreting the complex cyclic behaviours characteristic of integral abutment bridge systems.

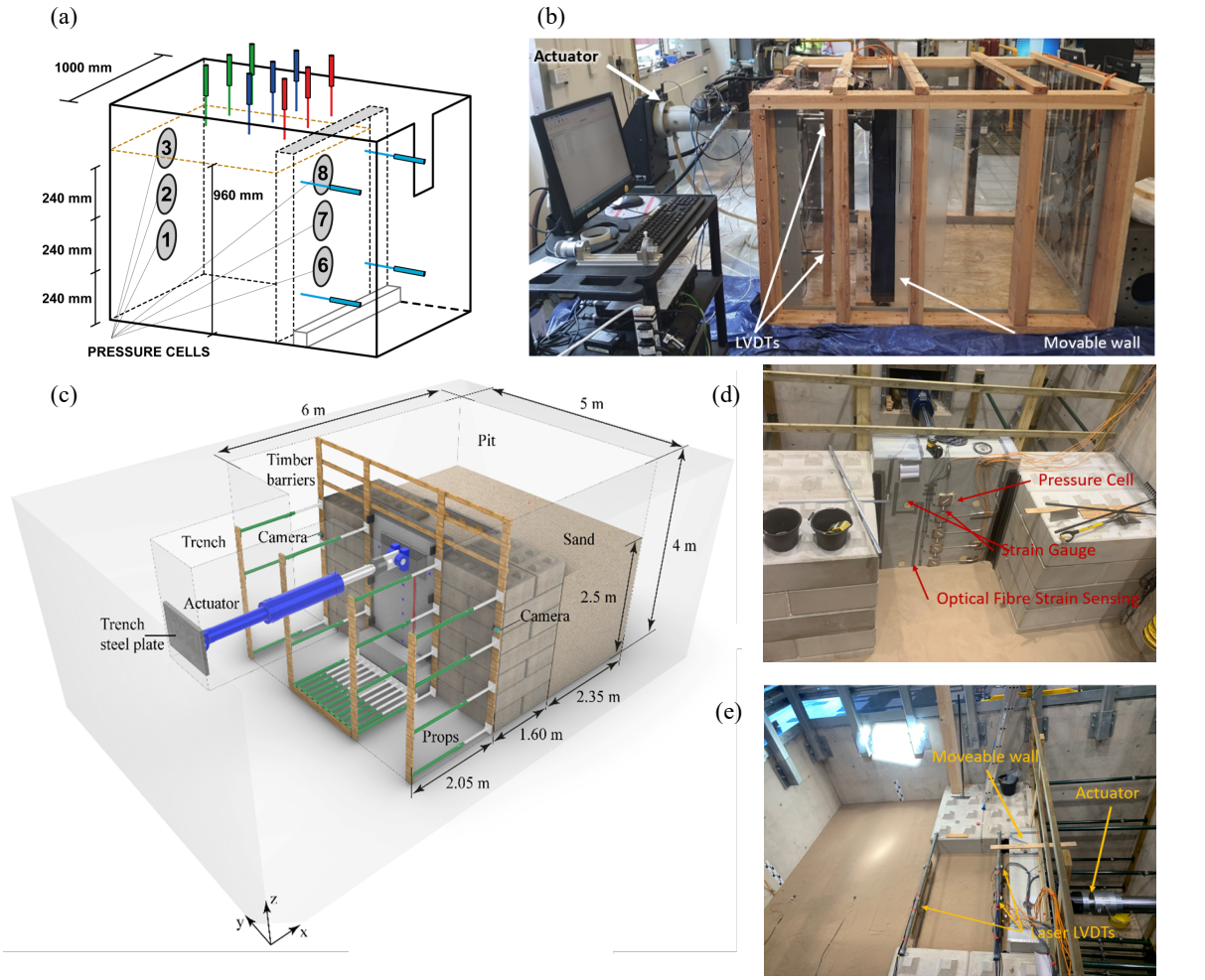

Figure 1. (a) Locations of pressure cells at the end wall (1–3) and moveable wall (6–8), along with LVDT placements (Source: Luo et al., 2023, Published by Elsevier Ltd under the CC BY license: http://creativecommons.org/licenses/by/4.0/). (b) Photograph of the small-scale 1g model setup during testing, illustrating the actuator, and data acquisition system. (c) Schematic of the large-scale physical model showing abutment dimensions, sand volume, actuator system, and sensor placements (Reproduced from Luo et al. (2025), with permission of Canadian Science Publishing). (d) Front view photo of the moveable wall. (e) Plan view photo of the test pit.

2.4 *Numerical Modelling Using PLAXIS, ABAQUS, OpenSees and MATLAB*

To complement and interpret the experimental findings, two types of numerical models were developed. First, finite element simulations were conducted using ABAQUS, PLAXIS 2D (Luo et al., 2023) and OpenSees (Huang et al. 2025). The ABAQUS model applied plane-strain elements to represent the soil–abutment system, using a Mohr–Coulomb model for the granular backfill. Cyclic horizontal displacements were applied to simulate seasonal thermal movements, and the model reproduced key trends such as pressure build-up, deformation localisation, and the influence of boundary stiffness. In parallel, a PLAXIS 2D model incorporating a hardening soil formulation was used to validate the observed stress redistribution and strain concentration. The OpenSees model was developed using the STKO interface to simulate the soil–abutment interaction observed in the 1g experiments. The abutment was represented using an elastic beam-column element, while the granular backfill was modelled with plane strain quadrilateral elements obeying the PressureDependMultiYield02 constitutive model. Interface behaviour was defined via EqualDOF constraints to enforce displacement compatibility. Building on these simulations, Luo et al. (2025) introduced a custom MATLAB-based numerical framework to investigate the cumulative effects of cyclic loading over a 120-year service life. The model included a void-ratio-based densification mechanism and non-linear pressure redistribution, enabling prediction of lateral stress build-up with progressive cycles.

3 RESULTS

3.1 *Lateral Earth Pressure Trends*

The evolution of lateral earth pressure under thermal loading was explored through both small-scale 1g tests and large-scale physical modelling. In the small-scale experiments, two key factors were found to influence lateral pressure development: the number of thermal cycles and the magnitude of cyclic displacement. At early stages, lateral pressures increased rapidly with number of cycles, but this growth gradually diminished, suggesting the presence of an upper bound. Likewise, larger displacement amplitudes led to higher peak pressures and more significant soil deformation behind the abutment.

Comparative tests on abutments with varying stiffness further revealed that rigid walls develop over 25% higher lateral pressures than their more flexible counterparts. This distinction is attributed to greater backfill densification against stiffer walls under repeated loading. Numerical modelling using PLAXIS and ABAQUS confirmed that these trends can be reproduced using Mohr–Coulomb soil models, particularly for flexible abutments. However, these models do not fully capture progressive cyclic densification effects.

Large-scale testing reinforced and extended these observations. Initially, lateral pressures were relatively low due to the loose condition of the backfill. As thermal cycles progressed, pressures intensified, particularly near the abutment wall. This increase is interpreted as resulting from gradual backfill densification under cyclic displacement. Numerical simulations showed good agreement with measured trends when soil behaviour was adjusted over time - from a loose, elastic–plastic profile in early cycles to a dense, nonlinear elastic–perfectly plastic response in later stages. Beyond 40 cycles, pressure development stabilized, with a linear elastic model providing an upper-bound approximation up to 120 cycles.

Together, these findings demonstrate that both cumulative displacement and the evolving density of the backfill play critical roles in governing lateral earth pressure variations. These effects must be accounted for in the design and assessment of integral bridge abutments to ensure long-term structural performance.

To better compare the magnitude and trends of lateral earth pressure across various test methods and numerical approaches, a summary of K_p values at peak lateral pressure locations is presented in Table 1. Here, K_p is defined as the ratio of horizontal earth pressure to vertical stress at the depth where the maximum lateral pressure occurs. Max d/H (%): The maximum imposed cyclic horizontal displacement at the abutment top, expressed as a percentage of wall height. Cycle: The range of loading cycles applied in each test or model. z/H: The backfill depth (z) over wall height (H) at which the peak lateral earth pressure was recorded. The table consolidates results from small-scale and large-scale tests, finite element models (PLAXIS, ABAQUS, OpenSees), analytical theories, and the UK design guideline PD6694-1. Across all entries, the assumed critical friction angle of the backfill ranged from 31° to 32°, depending on the sand state (loose or densified). In small-scale and numerical tests using Mohr–Coulomb material models, 32° was consistently applied to represent medium-dense sand. In analytical and large-scale modelling cases, a slightly lower value (31°) was adopted.

Evidently, the rigid wall configurations consistently produced higher K_p values - reaching up to 9.8 - particularly in early-cycle ranges, which is attributed to more effective backfill confinement and densification under thermal movement. In comparison, flexible walls exhibited slightly lower peak pressures, though the K_p values remained significantly higher than those predicted by static design methods, confirming the cumulative effect of cyclic displacement on pressure build-up. Large-scale physical testing showed a clear increase in K_p from 4.2 during early cycles to 9.6 in later stages (cycle #10 to #120), further validating the progressive stiffening of the backfill with repeated thermal loading. Numerical models, such as those developed in MATLAB, successfully captured this trend by adjusting soil parameters - representing loose sand in early cycles ($K_p \approx 5$) and densified sand later ($K_p \approx 6.8$). Among the numerical formulations, the OpenSees model, using a plasticity-based PressureDependentMultiYield02 material, yielded one of the highest K_p values (9.8) at a shallow depth (z/H = 0.46), demonstrating the model's sensitivity to soil properties evolution and cyclic accumulation. By contrast, the PD6694-1 design code and classical analytical theories, such as Rankine and Coulomb, predicted much lower values in the range of 3.1 to 3.9, as they do not incorporate cyclic effects or backfill densification.

Table 1. Summary of the depth ratio where peak lateral earth pressure was observed, and corresponding K_p values from various test types, numerical models, design code and analytical methods.

Test Type / Model	Max d/H (%)	Cycle	z/H	K_p
Small-Scale Test - Flexible Wall	±3.45	1-12	0.5	7.2
Small-Scale Test - Rigid Wall	±3.45	1-12	0.5	8.2
Numerical - PLAXIS - Flexible Wall - FE	±3.45	1-12	0.6	6.5
Numerical - PLAXIS - Rigid Wall - FE	±3.45	1-12	0.8	9.6
Numerical - ABAQUS - Flexible Wall – FE	±3.45	1-12	0.5	7.2
Numerical - ABAQUS - Rigid Wall - FE	±3.45	1-12	0.8	8.4
Numerical - OpenSees - Rigid Wall - FE	±3.45	1-12	0.46	9.8
PD6694-1 (UK Design Code)	±3.45	N/A	0.5	4.6
Large-Scale Test - Concrete Wall (Early)	±0.48	1-10	0.64	4.2
Large-Scale Test - Concrete Wall (Rest)	±0.48	10-120	0.5	9.6
Numerical - MATLAB Model - Concrete Wall	±0.48	N/A	0.57	6.8
Numerical - MATLAB Model - Concrete Wall	±0.48	N/A	0.48	5
Rankine Analytical	N/A	N/A	N/A	3.1
Coulomb Analytical	N/A	N/A	N/A	3.9

The code approach based on PD6694 allows the evaluation of the design value of the earth pressure coefficient for expansion K_d^* can be estimated from equation 1, but should not be taken as greater than $K_{p;t}$: for full height abutments on spread footings.

$$K_d^* = K_0 + (\frac{C d_d'}{H})^{0.6} K_{p;t} \quad (1)$$

Where K_0 is the coefficient of earth pressure at rest; H is the vertical distance from ground level to the level at which the abutment is assumed to rotate; d_d' is the wall deflection at depth $H/2$ below ground level; C is 20 for foundations on flexible (unconfined) soils with Young's modulus of the ground (E) ≤ 100 MPa, it is 66 for foundations on rock or soils with E ≥ 1000 MPa, it may be found by linear interpolation for values of E between 100 MPa and 1000 MPa; $K_{p;t}$ is a coefficient of passive earth pressure used in the calculation of K_d^*. Note the

value (4.6) presented in the Table 1 below is the value of $K_{p;t}$, which is calculated based on the detail case in Luo et al (2025) from Table 8 in PD6694; while in there the K_d^* is around 1.4.

These comparative insights illustrate the limitations of static or simplified models in capturing the evolution of lateral earth pressures under repeated thermal loading. The progression from lower to higher K_p values across cycles underscores the importance of incorporating soil state transitions and cumulative displacement effects into design methods for integral bridge abutments.

3.2 *Soil Densification and Loosening*

Evidence from GPR scans and embedded instrumentation revealed non-uniform changes in soil compaction under repeated thermal loading. Surface zones generally exhibited loosening due to tensile strains during expansion phases, while deeper layers densified under sustained compressive effects. This stratified compaction pattern was observed consistently in both small- and large-scale experiments. The trends were found by temporal changes in signal velocity from GPR data. Notably, the evolution of GPR velocity in the small-scale test showed progressive deep-layer densification and surface loosening as the number of cycles increased.

Table 2 summarises these changes by correlating depth zones with percentage changes in GPR velocity over selected thermal loading cycles. Positive values represent increasing velocity (indicative of densification), while negative values reflect decreasing velocity (indicative of loosening). This progression underscores a growing compaction gradient with cyclic loading.

Table 2. GPR-Derived Velocity Changes During Thermal Cycles in Small-Scale Test

Cycle Count	Depth (m) Range	Velocity Change Trend (%)	Interpretation
20	0–0.3	+10 to +30	Deep layer densification begins
	0.7–1.0	–10 to –30	Surface loosening observed
40	0–0.3	+10 to +25	Continued deep compaction
	0.7–1.0	–10 to –25	Surface layer loosening continues
60	0–0.3	+10 to +20	Stable densification zone formed
	0.7–1.0	–10 to –20	Sustained loosening
80	0–0.3	+15 to +25	Deep zone increasingly compacted
	0.7–1.0	–15 to –20	Upper layer loosening enhanced
120	0–0.3	+20 to +30	Strong densification near base
	0.7–1.0	–15 to –30	Surface loosening well-established

Note: Negative values indicate velocity reduction (loosening); positive values indicate velocity increase (densification).

These observations from GPR were further supported by PIV analysis of small-scale tests (Luo et al., 2022), which revealed consistent trends in volumetric strain and deformation direction under repeated thermal loading. In tests with a rigid abutment, higher soil contraction was observed near the abutment interface during extension phases, while in more flexible configurations, greater deformation occurred during contraction phases. Additionally, tests on the rigid abutment showed rapid densification of the backfill within the first two loading cycles, which gradually diminished in later cycles. This behaviour confirms that backfill compaction is not only dependent on abutment stiffness, but also decreases in rate with increasing thermal loading cycles. Together, the GPR and PIV findings reinforce a layered compaction pattern and highlight the key influence of stiffness and loading history on soil-structure interaction.

These measured patterns of stratified soil behaviour help explain the observed evolution and distribution of lateral earth pressures discussed in Section 3.1. The deep-layer densification captured through GPR velocity increases corresponds to zones where peak lateral pressures were recorded, particularly in the lower half of the wall (e.g., z/H ≈ 0.46–0.64). Naturally, as soil compacts under repeated cyclic loading, its resistance to lateral movement increases, resulting in a higher K_p value at these depths. In contrast, surface loosening reduces confinement near the top, aligning with the relatively lower pressures measured in upper zones. This layered behaviour explains both the rising magnitude and shifting location of maximum lateral pressures with increasing cycles, reinforcing the strong coupling between soil state transitions and pressure distribution in integral bridge backfills.

4 IMPLICATIONS FOR PD 6694 AND FUTURE DESIGN PRACTICE

The experimental and numerical findings presented in this study challenge fundamental assumptions embedded in current design guidance, particularly PD 6694-1, which prescribes simplified static lateral pressure distributions for integral abutments. Observed cyclic soil–structure interaction responses reveal a more complex and temporally evolving behaviour, warranting a shift in both analytical frameworks and code development strategies.

4.1 *Reassessment of Lateral Earth Pressure Assumptions and Backfill Response*

Empirical data from small- and large-scale thermal cyclic tests demonstrate pronounced lateral earth pressure accumulation, particularly at mid-depth and base locations of the abutment wall. These results deviate from the canonical triangular stress profile assumed in PD 6694-1 (BSI, 2011), revealing a depth-dependent and non-monotonic pressure evolution. Notably, the small-scale models exhibited peak lateral pressure ratios near the upper zones, whereas the large-scale experiments showed pressure peaks shifting toward mid-height-aligning more closely with code expectations but exceeding prescribed magnitudes.

Such discrepancies underscore the influence of structural stiffness, boundary constraints, and scale-dependent soil mechanics on backfill stress trajectories. Importantly, embedded distributed fibre optic sensors captured heterogeneous densification trends with increasing thermal cycles, indicating that backfill compaction and stress redistribution are both spatially variable and cumulative. These findings suggest that PD 6694 should be revised to incorporate dynamic lateral pressure evolution, scale-sensitive effects, and long-term cyclic mechanisms that more accurately reflect in-service conditions.

4.2 *Advancing Performance-Based Frameworks through Scalable Monitoring*

The integration of scalable, non-invasive sensing technologies, such as GPR and distributed optical fibre systems, offer a robust pathway for transitioning toward performance-based design paradigms. These methods have demonstrated the capacity to detect temporal and spatial variations in backfill density, stress

redistribution, and the onset of anomalies such as localised voids. Their concurrent use in multi-scale testing confirms their applicability across contexts, providing a means of both model validation and long-term structural health assessment.

Embedding such sensing strategies within the design and operational phases of integral bridges facilitates an adaptive infrastructure management model. This evolution would enable design standards like PD 6694 (BSI, 2011) to move beyond static assumptions, incorporating in situ measurements and real-time performance data to inform responsive design iterations and predictive maintenance planning.

5 CONCLUSIONS

This study investigated the evolution of lateral earth pressures on integral bridge abutments subjected to thermal cyclic loading, combining small-scale 1g tests, large-scale physical modelling, and numerical simulations. Key factors influencing lateral pressure development were identified as the number of thermal cycles, the magnitude of cyclic displacement, and the structural stiffness of the abutment. Rigid abutments consistently produced higher K_p values, highlighting their greater potential to mobilise backfill confinement and densification under repeated loading.

Experimental results demonstrated that lateral pressures increase progressively with loading cycles but tend to stabilise beyond a certain threshold, reflecting backfill densification and stress redistribution. A clear upward trend in K_p values was observed - from 4.2 in early cycles to over 9.6 after 120 cycles - emphasising the evolving soil-structure interaction. Classical theories and design codes, such as Rankine, Coulomb, and PD6694-1, were shown to underestimate these pressures, as they do not account for cyclic effects or soil state transitions.

Validation through GPR and PIV data provided direct evidence of local density changes, supporting the interpretation that backfill densification significantly contributes to aggravating lateral earth pressures. The location of peak lateral pressure was found to shift as a function of soil compaction, typically occurring at mid-depth to the lower third of the wall.

The findings underline the need for updated design approaches that integrate cumulative displacement effects and evolving soil states. Incorporating such considerations can improve long-term performance predictions of integral bridge abutments, especially in climates with significant temperature variations.

6 ACKNOWLEDGEMENTS

This research was funded by the UK Engineering and Physical Sciences Research Council via its support for the UK Collaboratorium for Research on Infrastructure and Cities (UKCRIC, Grant Ref. EP/R017727) and specifically UKCRIC PLEXUS (Priming Laboratory EXperiments on infrastructure and Urban Systems, Grant Ref. EP/R013535), the UKCRIC PLEXUS Plus project, UKCRIC NBIF (Grant Ref. EP/P013635) and UKCRIC SoFSI (Grant Ref. EP/R012806/1). The authors are grateful for this funding and equally for the broader thinking on infrastructure systems provided by our UKCRIC colleagues.

7 REFERENCES

Barker, K.J., and Carder, D.R. 2000. Performance of the two integral bridges forming the A62 Manchester Road Overbridge. *Transport Research Laboratory*, Crowthorne, UK, TRL Report. p. 436

BSI. 2011. PD 6694-1:2011: recommendations for the design of structures subject to traffic loading to BS EN 1997-1. BSI, London, UK.

Burke, M.P., Jr 2009. *Integral and semi-integral bridges*. John Wiley Sons

Caristo, A., Barnes, J., and Mitoulis, S.A. 2018. Numerical modelling of integral abutment bridges under seasonal thermal cycles. *Proceedings of the Institution of Civil Engineers: Bridge Engineering*, 171(3):179–190.

Dicleli, M., and Erhan, S. 2010. Effect of soil–bridge interaction on the magnitude of internal forces in integral abutment bridge components due to live load effects. *Engineering Structures*, 32(1): 129–145. ISSN 0141-0296. doi:10.1016/j.engstruct.2009.09.001.

England, G.L., Tsang, N.C.M., and Bush, D.I. 2000. *Integral bridges: a fundamental approach to the time–temperature loading problem*. Thomas Telford, London, UK.

Fleming, P.R., and Rogers, C.D.F. 1995. Assessment of pavement foundations during construction. *Proceedings of the Institution of Civil Engineers-Transport*, 111: 105–115. doi:10.1680/itran.1995.27578.

Huang, Z., Fiorentino, G., Luo, S., De Risi, R., Metje, N., Chapman, D., ... & De Luca, F. (2025). Small-Scale PLEXUS 1g Tests on Integral Abutment Bridges: OpenSees Numerical Modelling. In: Lu, X., Demartino, C., Di Trapani, F., Lin, K., Monti, G. (eds) Proceedings of the 2024 Eurasian OpenSees Days. EOS 2024. Lecture Notes in Civil Engineering, vol 638. Springer, Cham.

Khodair, Y.A., and Hassiotis, S. 2005. Analysis of soil–pile interaction in integral abutment. *Computers and Geotechnics*, 32(3): 201–209. doi:10.1016/j.compgeo.2005.01.005.

LaFave J.M., Brambila G., Kode U., Liu G., Fahnestock L.A. 2021. Field behavior of integral abutment bridges under thermal loading. *Journal of Bridge Engineering*, 26(4): 04021013.

Lawver, A., French, C., and Shield, C.K. 2000. Field performance of integral bridge. Transportation Research Record: *Journal of the Transportation Research Board*, 1740: 108–117. doi:10.3141/1740-14.

Lehane, B.M. 2011. Lateral soil stiffness adjacent to deep integral bridge abutments. *Géotechnique*, 61(7): 593–603. doi:10.1680/geot.9.P.135.

Liu H., Han J., Parsons R.L. 2022. Settlement and horizontal earth pressure behind model integral bridge abutment induced by simulated seasonal temperature change. *Journal of Geotechnical and Geoenvironmental Engineering*, 148(6).

Luo, S., De Luca, F., De Risi, R., Le Pen, L.,Watson, G.,Milne, D., et al. 2022. Challenges and perspectives for integral bridges in the UK: PLEXUS small-scale experiments. *Proc Inst Civil Eng-Smart Infrastruct Construct*, 175(1): 27–43.

Luo, S., De Risi, R., De Luca, F., Mylonakis, G., Harkness, J., Milne, D., Williams, D., Fiorentino, G., Metje, N., Chapman, D., Powrie, Rogers, C.W., and Sextos., A. 2025. Effect of cyclic thermal loading on the behaviour of integral abutment bridges: a large-scale experimental study in a soil pit. *Canadian Geotechnical Journal*. 62: 1-20. https://doi.org/10.1139/cgj-2024-0543

Luo, S., Huang, Z.Y., Asia, Y.Z., De Luca, F., De Risi, R., Harkness, J., et al. 2023. Physical and numerical investigation of integral bridge abutment stiffness due to seasonal thermal loading. *Transportation Geotechnics*, 42: 101064. ISSN 2214-3912. doi:10.1016/j.trgeo.2023.101064.

Mark, T. 2013. Measuring soil pressure within a soil mass. *Canadian Geotechnical Journal*. 50(7): 716–722. doi:10.1139/cgj-2012-0347.

Ravjee, S., Jacobsz, S.W., Wilke, D.N., and Govender, N. 2018. Discrete element model study into effects of particle shape on backfill response to cyclic loading behind an integral bridge abutment. *Granular Matter*, **20**: 68. doi:10.1007/s10035-018-0840-z.

Springman S.M., Norrish A.R.M., Ng C.W.W. 1996. Cyclic loading of sand behind integral bridge abutments. *Transport Research Laboratory*, Crowthorne, UK, TRL Report. p. 146.

Tapper L., Lehane B. 2004. Lateral stress development on integral bridge abutments.*In Developments in mechanics and structures of materials*. *Edited by* Deeks A.J., Hao H. Perth, Australia edn. vol. 2. CRC Press/Balkema, the Netherlands. pp. 1069–1075.

Xu, M., and Guo, J. 2021. DEM study on the development of the earth pressure of granular materials subjected to lateral cyclic loading. *Computers and Geotechnics*, 130: 103915. ISSN 0266-352X. doi:10.1016/j.compgeo.2020.103915.